Observation of an Energetic Radiation Burst from Mountain-Top Thunderclouds

H. Tsuchiya,[1] T. Enoto,[2] T. Torii,[3] K. Nakazawa,[2] T. Yuasa,[2] S. Torii,[2] T. Fukuyama,[2] T. Yamaguchi,[2] H. Kato,[1]
M. Okano,[1] M. Takita,[4] and K. Makishima[1,2]

[1]*Cosmic Radiation Laboratory, Riken, 2-1, Hirosawa, Wako, Saitama 351-0198, Japan*
[2]*Department of Physics, University of Tokyo, 7-3-1, Hongo, Bunkyo-ku, Tokyo 113-0033, Japan*
[3]*Tsuruga Head Office, Japan Atomic Energy Agency, 2-1, Shiraki, Tsuruga, Fukui 919-1279, Japan*
[4]*Institute for Cosmic Ray Research, University of Tokyo, Kashiwa, Chiba, 277-8582, Japan*
(Received 24 January 2009; published 23 June 2009)

During thunderstorms on 20 September 2008, a simultaneous detection of γ rays and electrons was made at a mountain observatory in Japan located 2770 m above sea level. Both emissions, lasting 90 sec, were associated with thunderclouds rather than lightning. The photon spectrum, extending to 10 MeV, can be interpreted as consisting of bremsstrahlung γ rays arriving from a source which is 60–130 m in distance at 90% confidence level. The observed electrons are likely to be dominated by a primary population escaping from an acceleration region in the clouds.

Introduction.—Energetic radiation bursts from thunderstorm activity have been observed by space observatories as well as ground-based detectors. Interestingly, these bursts appear to be classified into two types according to their duration. One comprises short bursts lasting for milliseconds or less, mainly observed from the upper atmosphere of the Earth [1,2], natural lightning discharges [3,4], and rocket-triggered ones [5–7]. Though not necessarily homogeneous, they generally occur in association with lightning discharges. The other consists of long bursts with a duration of a few seconds to a few minutes, mostly detected at aircraft altitudes [8,9], at high mountains [10–14], and around the coastal area of the Japan Sea [15,16]. Unlike the short bursts, few of them appear to be clearly associated with lightning discharges.

To date, at least some of these radiation bursts are thought to result from relativistic electrons, which are produced in turn by a mechanism involving runaway and avalanches of electrons in the atmosphere. The mechanism, first proposed by Gurevich *et al.* [17], needs intense electric fields, high-energy seed electrons, and spatial length long enough for the avalanches to develop. When these conditions are fulfilled, the electrons can gain energy from the electric fields fast enough to exceed their ionization loss. Then, they will be accelerated to relativistic energies, and produce bremsstrahlung γ rays.

Actually, γ-ray spectra extending to ~10 MeV have been observed from both short and long bursts [2,7,16], with their properties generally consistent with the bremsstrahlung emission scenario. However, according to Monte Carlo simulations considering a feedback mechanism in which backscattered photons and/or positrons successively supply seed electrons in the high-electric-field region, electron avalanches are likely to last only for microseconds [18–20]. Observationally, only a few examples of long bursts have so far been reported to extend

to MeV energies. Therefore, it is not yet clear whether the runaway electron avalanche scenario, which is generally successful on some short bursts [2,7], can also explain the prolonged events. Furthermore, we need to explain the fact that some long bursts consist solely of x or γ rays [8–12,15,16], while others involve only charged particles [13,14]. Here, utilizing a detector that is capable of separating photons from charged particles, we first report on a simultaneous detection of γ rays and electrons in one long burst, with the photon spectrum extending to 10 MeV.

Experiment.—The Norikura cosmic-ray observatory ($36°6'$N, $137°33'$E), belonging to the Institute for Cosmic Ray Research, the University of Tokyo, is located on a high mountain in Gifu prefecture, Japan. Because of its high altitude, 2770 m above sea level, as well as meteorological conditions from summer to autumn, the observatory is frequently shrouded in thunderclouds.

Outside the observatory, we installed a radiation detection system on 4 September 2008, and operated it until 2 October 2008. The system consists of a spherical NaI scintillator with a diameter of 7.62 cm, and a $45 \times 40 \times 0.5$ cm^3 plastic scintillator which is enclosed in an aluminum box with the top and bottom being 1 and 3 mm thick, respectively. Each scintillator has a photomultiplier (HAMAMATSU R878) of its own, and each output signal is fed to a self-triggering electronics system, incorporating a 12 bit analog-to-digital converter (ADC). The detected events are collected in the order of arrival without individual arrival-time information, and recorded every 1 sec synchronized by Global Positioning System. Thus, both scintillators have a time resolution of 1 sec. The NaI scintillator was operated over 10 keV–12 MeV, while the plastic scintillator, placed above it, was operated with a threshold energy deposit of 500 keV.

The plastic scintillator has a high sensitivity for charged particles while it is much less sensitive to photons.

Therefore, when the NaI detector is triggered by an incident particle without a coincident (within $0.7~\mu\sec$) signal in the plastic scintillator, the incident particle would be a photon, not a charged particle. Thus, the plastic signals mainly represent incoming charged particles including electrons, and using them in anticoincidence, the NaI signals can be considered to indicate γ rays with little ($\sim 0.1\%$) contamination by electrons.

Aiming at an independent radiation observation, we installed, inside the observatory, another inorganic scintillation detector. This indoor detector uses a cubic bismuth germanate (BGO) scintillator of $5 \times 5 \times 15$ cm^3, which is coupled to a photomultiplier (HAMAMATSU R7600U-203), and observes in the 100 keV–5 MeV range. The signal is pulse-height analyzed by a self-triggering 8 bit ADC, and the pulse height is recorded, on an event-by-event basis, with arrival-time information of 20 ms resolution.

In addition to the radiation observations, we measure optical and electric field variations outside the observatory. The visible-light intensity is measured by an optical sensor using a photodiode (HAMAMATSU S1226-8BK) having a sensitivity to photons with wavelength of 320–1000 nm, with its peak at 750 nm. Output signals of this optical sensor are fed to a 12 bit ADC every 1 sec, and recorded as voltages between 0 and $+10$ V with a resolution of 5 mV. The electric field is measured by a commercial electric field mill (BOLTEK EFM-100). Its outputs are also collected by a 12 bit ADC every 1 sec, and converted to the electric field strength between ± 100 kV m^{-1} with a resolution of 50 V m^{-1}.

Results.—Examining the data over a period of 4 September to 2 October, we found a long-duration enhancement during thunderstorms on 20 September, but found no other events of similar properties. Figure 1 shows count histories of >10 keV NaI and >500 keV plastic scintillators, between 15:15 and 16:15 UT on 20 September. Besides gradual count-rate changes mainly due to Radon rain outs, both scintillators detected a significant count enhancement, or a burst, over a 90 sec interval of 15:45:10–15:46:40 UT. Excluding the data obtained in this interval and applying a quadratic least square fitting to the remaining data, we estimated background (solid curves in Fig. 1) in the two scintillators. Subtracting the interpolated background from the total observed counts in the 90 sec period and calculating the background errors using the derived quadratic function and the number of bins used in the fit procedure, 117, both NaI and plastic scintillators gave highly significant increases of $1208 \pm 150(8.1\sigma)$ and $658 \pm 104(6.3\sigma)$, respectively.

Figure 2 gives details of the count histories of the NaI scintillator, together with outputs of the electric field and light sensors. Since the plastic scintillator signals are used here in anticoincidence, the NaI events are thought to represent energetic photons. The excess counts in the
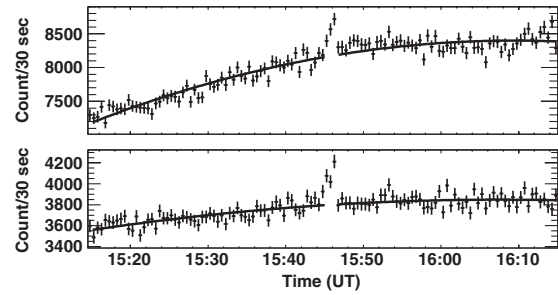

FIG. 1. Count rates per 30 sec of >10 keV NaI (top) and >500 keV plastic (bottom) scintillators between 15:15 and 16:15 UT on 20 September 2008. The horizontal axis represents universal time, and all errors are statistical 1σ. Each solid curve shows estimated background level.

0.01–3 MeV and 3–12 MeV bands [Figs. 2(a) and 2(b)] become 1033 ± 159 and 91 ± 15, respectively, while those without anticoincidece in the two energy bands are 1030 ± 159 and 92 ± 16, respectively. Since the excess counts with and without the anticoincidence thus statistically agree, we infer that the NaI signals were dominated by photons, not charged particles.

On this occasion, the indoor BGO detector also showed a moderate increase in >2.6 MeV energies, with a $\sim 4\sigma$ significance when summed over a 15 sec interval. The absolute time of this increase is consistent with that in the outdoor detector, within a relatively large uncertainty
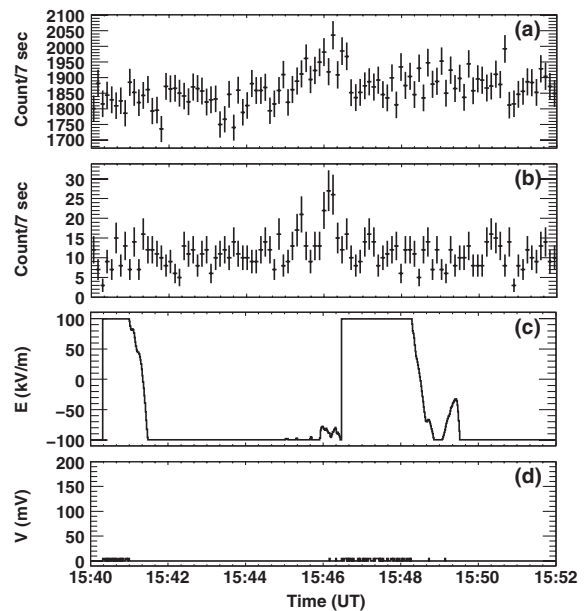

FIG. 2. Detailed count histories of the NaI counter with anti-coincidence, and the electric field and light sensors, between 15:40 and 15:52 UT. All abscissa are universal time. Panels (a) and (b) show count histories per 7 sec of the NaI counter in 0.01–3 MeV and 3–12 MeV energies, respectively, with 1σ statistical errors. (c) One-second electric field data variations. (d) One-second optical data outputs.

of 3 min with which the clock of the data-taking computer of the indoor detector was adjusted. Supposing that the outdoor and indoor detectors observed the same event, the lower significance in the latter, compared to the former, suggests that the burst source was located outside the building, and the radiation was attenuated by the roofs and/or walls.

Because of a limited dynamic range of the electric field mill, the electric field [Fig. 2(c)] was saturated at -100 kV m^{-1} at 15:45:10 UT (burst onset), and kept negative polarity until 15:46:29 UT. At that time, the electric field rapidly changed its polarity from negative to positive within 1 sec, and saturated at $+100 \text{ kV m}^{-1}$. However, the outputs of the optical sensor [Fig. 2(d)] remained at 0 mV which is typical at midnight (15:00 UT corresponds to local midnight): its small fluctuations, ~ 5 mV, reflect the ADC resolution. In reality, when the optical sensor detects lightning, it typically records a few hundred mV or even >5 V on rare occasions. Thus, we conclude that no lightning occurred during the burst, and hence this burst is associated with thunderclouds.

Figure 3(a) shows the background-subtracted photon spectrum, summed over the burst period (90 sec). Here, we subtracted a background spectrum averaged over 15:30–15:40 UT and 15:50–16:00 UT, when the thunderstorm was ongoing. This is to remove effects of Radon rain outs, which gradually increased the <3 MeV background up to twice those in quiescent periods. The resultant background-subtracted spectrum exhibits a very hard continuum, clearly extending to 10 MeV.

We can estimate the initial photon energy spectrum at the source, from the background-subtracted spectrum. Theoretically, the number of nonthermal bremsstrahlung photons per unit energy emitted by monochromatic electrons is in inverse proportion to the photon energy, up to energies which are close to the electron energy [21]. Also,
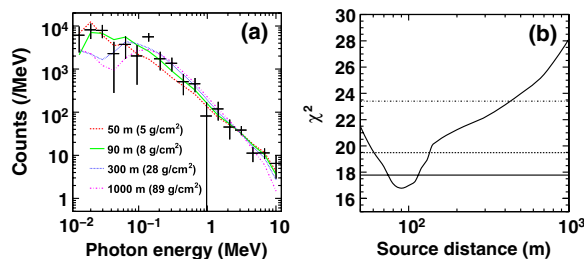

FIG. 3 (color online). (a) The background-subtracted photon energy spectra (black points) obtained from the NaI signals with anticoincidence. The horizontal and vertical axes represent the photon energy and the counts per energy bin, respectively. Error bars are statistical 1σ. Each curve shows prediction of an incident power-law model. Air mass in g cm^{-2} corresponding to the assumed source distance is shown in parentheses. (b) The χ^2 value of the model fit to the data, plotted against the assumed source distance. Horizontal lines from bottom to top represent 68%, 90%, and 99% confidence levels.

a numerical simulation [22] has shown that a population of rather flat power-law distributed, or even monochromatic, relativistic electrons colliding with a thick medium produces a power-law bremsstrahlung photon spectrum with a very hard photon index. Thus, we simply assume that the initial photon spectrum is a power law of the form $\alpha E^{-\beta}$, where α is a normalization factor (photons $\text{MeV}^{-1} \text{ sr}^{-1}$), β is the photon index, and E is the photon energy in MeV. Then, to derive the photon energy spectra to be observed at the observatory, we simulated the photon propagation in the atmosphere with CORSIKA 6.500 [23] incorporating EGS4 [24] to correctly treat electromagnetic interactions in relatively low energies relevant to the present work. The photons were assumed to be injected vertically into the atmosphere, and to propagate while suffering Compton scattering and other processes. Finally, the simulated arrival photon spectra, after convolving with the detector response, were fitted to the observed photon spectrum in search for the best-fit values of α and β for various source distances assumed. The predicted spectra for representative source distances up to 1000 m are shown in Fig. 3(a); larger distances give poorer fits (e.g., $\chi^2 = 42.2$ for 3000 m). From Fig. 3(b), the source distance, $d = 90$ m, gives the minimum $\chi^2/(\text{degrees of freedom}) = 16.8/16$, with $\alpha = (2.4 \pm 0.4) \times 10^8 \text{ MeV}^{-1} \text{ sr}^{-1}$ and $\beta = 1.15 \pm 0.09$ (quoted errors are 90% confidence values). Figure 3(b) also gives a constraint as $d = 60$–130 m at 90% confidence level.

Discussion.—The present γ-ray burst is not due to Radon or its daughters, because the γ rays related to Radon have energies of 0.1–2 MeV, and last for a much longer time [10]. Compared with some prolonged intracloud x-ray emissions [8,9], this burst strongly suggests that electrons were accelerated beyond 10 MeV in thunderclouds. Furthermore, the most outstanding difference of the present burst from previous ones [8–16] is that charged particles, most likely electrons, were simultaneously observed. This difference may be attributable to the short distance, ~ 90 m, of the present event. Actually, 20 (10) MeV electrons have a range of 110 (60) m at an altitude of 2770 m, which is in good agreement with the constraint on d derived above.

We can construct the following picture of the present event. As predicted by Gurevich *et al.* [17], seed electrons with energies of >100 keV, produced by, e.g., cosmic rays, are electrostatically accelerated in thunderclouds to relativistic energies, and are multiplied therein. We may expect the electron spectrum to reach ~ 20 MeV, because a numerical study [25] predicts that the runaway electrons have an average kinetic energy of ~ 7 MeV with a spread of ~ 12 MeV. The 20 MeV electrons can effectively emit bremsstrahlung γ rays extending to 10 MeV, and escape from the thunderclouds to propagate a distance of ~ 90 m, with their energies reducing down to a few MeV. Because of a Compton optical depth of 0.51 (0.12) at 1 (10) MeV for

$d = 90$ m, the emitted γ rays are sometimes scattered by large angles with significant energy loss, producing secondary electrons.

If the primary electrons were in a perfect parallel beam, relativistic effects would make the emitted γ rays, especially high-energy ones, mostly beamed into a forward narrow cone with a half-opening angle of $\Gamma^{-1} \sim 1.5°$, where $\Gamma = 40$ is the Lorentz factor of 20 MeV electrons. In practice, the cone will be much broader, due to multiple scatterings of the emitting electrons, and to the mild Compton scatterings of the emitted photons. The γ-ray spectrum is expected to be hardest along the cone axis. Since the observed spectrum clearly extends to 10 MeV, it is thought that a rather harder part of the γ-ray emissions was detected. In particular, the derived photon index, 1.15 ± 0.09, is close to the theoretically hardest limit (1.0). Thus, we infer that our detectors viewed the cone nearly along its axis.

We may estimate how the Compton-scattered electrons and the escaping primary ones contribute to the excess counts detected by the plastic scintillator, $N_{ob} = 658 \pm 104$. According to a Monte Carlo simulation, the survival probability of >1 MeV (at the detector) secondary electrons, produced by 3, 5, and 10 MeV γ rays propagating from a source at $d = 90$ m, are 0.01, 0.02, and 0.04, respectively. Thus, employing the photon spectrum at $d = 90$ m, $f_{90}(E) = 2.4 \times 10^8 E^{-1.15}$, the expected count of the >1 MeV secondary electrons in the plastic scintillator becomes at most $n_{se} \sim 110$ even if all the scattered electrons with arriving energies of >1 MeV are collected: we neglected lower-energy ones, since ionization losses in the 1 mm thick aluminum window prevents them from depositing >500 keV energies in the plastic scintillator. Hence, we presume that the escaping primary electrons contribute to N_{ob} by $N_d = N_{ob} - n_{se} = 548 \pm 104$.

From this N_d, we can evaluate the total number of 20 MeV primary electrons for $d = 90$ m as

$$N_{20} = N_d d^2 / (S\epsilon) \sim 3.1 \times 10^8, \tag{1}$$

where $S = 1800$ cm^2 represents the area of the plastic scintillator, and $\epsilon \sim 0.08$ denotes the attenuation factor of >1 MeV electrons in the atmosphere and the aluminum window. Using this N_{20} and the initial photon spectrum $f_{90}(E)$, the spatial vertical length of the acceleration region, needed for the accelerated electrons to produce the observed bremsstrahlung γ rays, can be estimated with an assumed beam half-opening angle θ_h as

$$H \sim 2\pi N_{20}^{-1} \int_0^{\theta_h} \int_1^{12} f_{90}(E)/\eta(E, \theta) \sin\theta \, dE \, d\theta, \tag{2}$$

where $\eta(E, \theta)$ is the probability per 1 g cm^{-2} with which the 20 MeV electrons emit bremsstrahlung photons with an energy E and an angle θ with respect to the cone axis [21]. At $\theta_h = 15°$, which is 10 times larger than the perfect parallel beam case (1.5°), the above H becomes 200 m, and

in turn gives the electrostatic potential difference in the acceleration region as $U = 200$ kV m$^{-1} \times 200$ m $= 40$ MV, where 200 kV m^{-1} is the critical electric field for seed electrons to cause the runaway electron avalanches given by $280P$ kV m^{-1} [20] with the atmospheric pressure $P = 0.72$ atm. This U is generally sufficient to accelerate high-energy seed electrons to relativistic energies or ~ 20 MeV if an electric field is higher than the critical value by 30%–40%. As discussed so far, this observation suggests that long-duration emissions of γ rays and electrons are due to relativistic runaway electrons, although other possibilities may not necessarily be excluded.

[1] G. J. Fishman *et al.*, Science **264**, 1313 (1994).
[2] D. M. Smith *et al.*, Science **307**, 1085 (2005).
[3] C. B. Moore *et al.*, Geophys. Res. Lett. **28**, 2141 (2001).
[4] J. R. Dwyer *et al.*, Geophys. Res. Lett. **32**, L01803 (2005).
[5] J. R. Dwyer *et al.*, Science **299**, 694 (2003).
[6] J. R. Dwyer *et al.*, Geophys. Res. Lett. **31**, L05118 (2004).
[7] J. R. Dwyer *et al.*, Geophys. Res. Lett. **31**, L05119 (2004).
[8] M. P. McCarthy and G. K. Parks, Geophys. Res. Lett. **12**, 393 (1985).
[9] K. B. Eack *et al.*, J. Geophys. Res. **101**, 29637 (1996).
[10] D. M. Suszcynsky, R. Roussel-Dupré, and C. Shaw, J. Geophys. Res. **101**, 23505 (1996).
[11] M. Brunetti *et al.*, Geophys. Res. Lett. **27**, 1599 (2000).
[12] A. P. Chubenko *et al.*, Phys. Lett. A **275**, 90 (2000).
[13] V. V. Alexeenko *et al.*, Phys. Lett. A **301**, 299 (2002).
[14] Y. Muraki *et al.*, Phys. Rev. D **69**, 123010 (2004).
[15] T. Torii, M. Takeishi, and T. Hosono, J. Geophys. Res. **107**, 4324 (2002).
[16] H. Tsuchiya *et al.*, Phys. Rev. Lett. **99**, 165002 (2007).
[17] A. V. Gurevich, G. M. Milikh, and R. Roussel-Dupre, Phys. Lett. A **165**, 463 (1992).
[18] J. R. Dwyer, Geophys. Res. Lett. **30**, 2055 (2003).
[19] L. P. Babich, E. N. Donskoy, and R. A. Roussel-Dupré, Geomagn. Aeron. **47**, 515 (2007).
[20] J. R. Dwyer, Phys. Plasmas **14**, 042901 (2007).
[21] H. W. Koch and J. W. Motz, Rev. Mod. Phys. **31**, 920 (1959).
[22] J. Kotoku *et al.*, Publ. Astron. Soc. Jpn. **59**, 1161 (2007).
[23] D. Heck *et al.*, Forschungszentrum Karlsruhe Report No. FZKA 6019, 1998.
[24] W. R. Nelson, H. Hirayama, and D. W. O Rogers, SLAC Report No. 265, 1985.
[25] R. Roussel-Dupré *et al.*, Space Sci. Rev. **137**, 51 (2008).